

Neutron star properties and the equation of state for its core

J. L. Zdunik, M. Fortin, and P. Haensel

N. Copernicus Astronomical Center, Polish Academy of Sciences, Bartycka 18, PL-00-716 Warszawa, Poland
jlz@camk.edu.pl, fortin@camk.edu.pl, haensel@camk.edu.pl

Received xxx Accepted xxx

ABSTRACT

Context. Few unified equations of state for neutron star matter where core and crust are described using the same nuclear model are available. However the use of non-unified equations of state with a simplified matching between the crust and the core has been shown to introduce uncertainties in the radius determination which can be larger than the expected precision of the next generation of X-ray satellites.

Aims. We aim at eliminating the dependence of the radius and mass of neutron star on the detailed model for the crust and on the crust-core matching procedure.

Methods. We solve the approximate equations of the hydrostatic equilibrium for the crust of neutron stars obtaining a precise formula for the radius which depends only on the core mass and radius, and on the baryon chemical potential at the core-crust interface and on the crust surface. For a fully accreted crust one needs additionally the value of the total deep crustal heating per one accreted nucleon.

Results. For typical neutron star masses the approximate approach allows to determine the neutron star radius with an error $\sim 0.1\%$ (~ 10 m, equivalent to a 1% inaccuracy in the crust thickness). The formalism applies to neutron stars with a catalyzed or a fully accreted crust. The difference in the neutron star radius between the two models is proportional to the total energy release due to deep crustal heating.

Conclusions. For a given model of dense matter describing the neutron star core, the radius of a neutron star can be accurately determined independently of the crust model with a precision much better than the $\sim 5\%$ one expected from the next generation of X-ray satellites. This allows to circumvent the problem of the radius uncertainty which may arise when non-unified equations of state for the crust and the core are used.

Key words. dense matter – equation of state – stars: neutron

1. Introduction

The interior of a neutron star (NS) consists of two main parts: the liquid core and the solid crust. While the core is uniform (homogeneous), the crust is non-uniform composed of nuclear clusters. Consequently, calculating the crust equation of state (EOS) is much less-straightforward than for the core, explaining the smaller number of crust EOS available compared to the ones for the core. In particular few unified EOS, i.e. based on the same nuclear model for the crust and core, have been developed, see eg. Douchin & Haensel (2001); Fantina et al. (2013); Pearson et al. (2014); Fortin et al. (2016). Therefore non-unified EOS are often used, assuming different nuclear interaction models for the crust and the core. As shown in Fortin et al. (2016), for masses of astrophysical interest ($M > 1 M_{\odot}$) the use of non-unified EOS can introduce an uncertainty on the radius determination of the order of 5%, as large as the precision expected from the next generation of X-ray telescopes: NICER (Arzoumanian et al. 2014), Athena (Motch et al. 2013) and potential LOFT-like missions (Feroci et al. 2012).

The solid crust of a NS with a mass $M > 1 M_{\odot}$ contains only about one percent of star's total mass. However, the crust is believed to play an important role in many NS phenomena, e.g. pulsar glitches, X-ray bursts, gamma-ray flares of magnetars, torsional oscillations of NS, cooling of

isolated NS, cooling of X-ray transients (for review see e.g. Chamel & Haensel 2008). A standard model of NS crust assumes that it is built of matter in nuclear equilibrium, the thermal corrections are negligibly small, and at a given baryon number density n , the crust matter is in a state of minimum energy per nucleon, E . In such a state which defines the ground state (GS) of matter, the matter is called *catalyzed*. As the density n (or the mass-energy density ρ) can undergo discontinuous jumps inside the NS, a more suitable independent variable is the pressure P , which is strictly monotonous within the star. The thermodynamic potential is then the Gibbs free energy (the baryon chemical potential) $\mu = E + P/n$ which replaces E . In the strict GS of matter both P and μ are continuous and monotonously increasing with the density when going towards the NS center.

The GS approximation is expected to be good for isolated NS born in core-collapse supernovae. However, a significant fraction of NS remains for $10^8 - 10^9$ yr in low-mass X-ray binaries (LMXB), where they undergo a phase of accretion of matter from its evolved companion star. During the LMXB stage the NS is spun-up to millisecond periods, this is the so-called pulsar recycling. In such accreting NS the original crust has been replaced (fully or partially) by an accreted one. In what follows we consider only a fully accreted crust, i.e. we assume that the NS has accreted matter with an integrated rest mass larger than the rest mass of the original GS crust.

Send offprint requests to: jlz@camk.edu.pl

The composition of an accreted crust (AC) is expected to be very different from the one of a crust built of catalyzed matter in the GS. However, the neutron drip, dividing the whole crust into the outer (nuclei in electron gas) and the inner (nuclei in neutron gas and electron gas) crusts is found at similar density for GS and AC cases. Chamel et al. (2015) find, using up-to-date energy density functionals and the Hartree-Fock-Bogoliubov method for solving the nuclear many-body problem, $\rho_{\text{ND}}^{(\text{GS})} = 4.3 - 4.4 \times 10^{11} \text{ g cm}^{-3}$. For an accreted crust they find some dependence on the energy density functional model, as well as on the initial composition of ashes of X-ray bursts, $\rho_{\text{ND}}^{(\text{AC})} = 2.8 - 6.1 \times 10^{11} \text{ g cm}^{-3}$.

The accreted crust is, in contrast to the GS one, a reservoir of the nuclear energy. This energy can be steadily released mainly at some 300 - 500 m below the NS surface, during the accretion phase, leading to *deep crustal heating* (Haensel & Zdunik 1990; Brown et al 1998). The EOS of an AC is stiffer than that for the GS crust, particularly for densities $5 \times 10^{11} - 5 \times 10^{12} \text{ g cm}^{-3}$. Consequently, the thickness of an AC is larger (Zdunik & Haensel 2011).

In the present paper we present an approximate description to the NS crust structure in terms of the function relating the chemical potential and the pressure. Within the one-component plasma model, we derive in Sect. 2 a formula for the thickness of any layer of the crust. It is highly accurate and does not require any knowledge of the EOS but the values of the chemical potential at the boundaries of a given layer in the crust. The approach is then extended to describe a GS crust and formulas for the NS radius, the crust thickness and mass depending only on the mass and radius of the NS core are obtained. Their accuracy and the dependence on the choice of the location of the core-crust transition are studied in Sect. 3. In particular it is shown that the radius and mass of a neutron star, the crust thickness and its mass can be determined with an error smaller than 0.1%, 0.3%, 1% and 5% respectively. In Sect. 4 the approximated approach is extended to the case of an accreted crust and a simple formula for the difference in the thickness of the AC and GS crusts is obtained. It only involves the total (integrated) energy release due to deep crustal heating, and the mass and radius of a NS with a GS crust and is extremely accurate ($< 1 \text{ m}$). Conclusions and perspectives are presented in Sect. 5.

2. Crust structure: an approximation

The approximate approach to the macroscopic properties of the NS crust based on the separation of the TOV equation into two factors dependent on stellar properties (mass and radius) and the EOS of dense matter was discussed in Lattimer & Prakash (2007); Zdunik (2002); Zdunik et al (2008); Zdunik & Haensel (2011).

The Tolman-Oppenheimer-Volkoff (TOV) equation of hydrostatic equilibrium in General Relativity is:

$$\frac{dP}{dr} = - \left(\rho + \frac{P}{c^2} \right) \left(1 - \frac{2Gm}{rc^2} \right)^{-1} \left(\frac{Gm}{r^2} + 4\pi Gr \frac{P}{c^2} \right) \quad (1)$$

with $m = m(r)$ the gravitational mass enclosed in a sphere of radius r , P the pressure and ρ the mass-energy density.

The mass of the crust M_{crust} being small compared to the total mass M of the NS, within the crust $m \approx M$ and

$4\pi r^3 P / mc^2 \ll 1$. Consequently Eq. (1) can be rewritten, in the crust¹:

$$\frac{dP}{\rho + P/c^2} = -GM \frac{dr}{r^2(1 - 2GM/rc^2)}. \quad (2)$$

Let P_{cc} , n_{cc} and $\mu_{\text{cc}} = \mu(P_{\text{cc}})$ be the pressure, baryon density and chemical potential at the core-crust interface, respectively. Within the crust, i.e. for $0 < P < P_{\text{cc}}$, we define a dimensionless function of the local pressure:

$$\chi(P) = \int_0^P \frac{dP'}{\rho(P')c^2 + P'}. \quad (3)$$

Notice that $\chi(P)$ is determined solely by the EOS of the crust. The integral of the right-hand side of Eq. (2) then becomes:

$$\chi[P(r)] = \frac{1}{2} \ln \left[\frac{1 - r_g/R}{1 - r_g/r} \right], \quad (4)$$

where $r_g \equiv 2GM/c^2$. Defining $a = 1 - r_g/R$, we obtain r within the crust as a function of χ :

$$r = r_g / (1 - ae^{-2\chi}). \quad (5)$$

In thermodynamic equilibrium one can define the baryon chemical potential $\mu = d\rho/dn$. Thus, the first law of thermodynamics at $T = 0$ implies:

$$\mu = \frac{P + \rho c^2}{n} \quad (6)$$

which leads to the relation

$$\frac{dP}{\rho c^2 + P} = \frac{dP}{d\mu} \frac{d\mu}{\rho c^2 + P} = \frac{d\mu}{\mu}. \quad (7)$$

The function χ is then given by $\exp(\chi) = \mu(P)/\mu_0$ where $\mu_0 = \mu(P = 0) = m_0 c^2$ is the energy per baryon at NS surface.

This allows to determine the thickness of any shell of the crust located between two radii r_1 and r_2 corresponding to the pressure P_1 and P_2 , respectively:

$$\frac{\sqrt{1 - 2GM/r_1 c^2}}{\sqrt{1 - 2GM/r_2 c^2}} = \exp(\chi_{1,2}) = \frac{\mu_2}{\mu_1}. \quad (8)$$

A similar approach presented by Lattimer & Prakash (2007) relies on the replacement of μ in the denominator of Eq. (7) by its value at the NS surface μ_0 leading to an exponential dependence in Eq. (8).

2.1. Approximate formula for the radius and crust thickness

Let R_{core} be the radius of the core, i.e. at the core-crust interface where $\mu = \mu_{\text{cc}}$. In Eq. (8), taking $r_1 = R$ and $r_2 = R_{\text{core}}$, one can obtain a formula relating $R(M)$ to $R_{\text{core}}(M)$:

$$\frac{\sqrt{1 - 2GM/Rc^2}}{\sqrt{1 - 2GM/R_{\text{core}}c^2}} = \frac{\mu_{\text{cc}}}{\mu_0}. \quad (9)$$

¹ The term $4\pi r^3 P / mc^2$ is of the order of $P/\rho c^2$ at the bottom of the inner crust but is three orders of magnitude smaller than $P/\rho c^2$ at the neutron drip point. This is the reason for keeping the factor $1 + P/\rho c^2$ while neglecting the term $4\pi r^3 P / mc^2$ as compared to one.

The latter is equivalent to:

$$\frac{2GM}{Rc^2} = \frac{2GM}{R_{\text{core}}c^2} - \left(\frac{\mu_{\text{cc}}^2}{\mu_0^2} - 1 \right) \left(1 - \frac{2GM}{R_{\text{core}}c^2} \right). \quad (10)$$

which expresses the compactness of the whole star in terms of the core compactness. Note that in this formula the EOS of the crust enters through the ratio μ_{cc}/μ_0 .

From Eq. (10) we find that the radius is given by:

$$R = \frac{R_{\text{core}}}{1 - (\alpha - 1)(R_{\text{core}}c^2/2GM - 1)} \quad (11)$$

where:

$$\alpha = \exp(2\chi) = \left(\frac{\mu_{\text{cc}}}{\mu_0} \right)^2. \quad (12)$$

Then the crust thickness $l_{\text{crust}} = R - R_{\text{core}}$ is:

$$l_{\text{crust}} = \phi R_{\text{core}} \frac{1 - 2GM/R_{\text{core}}c^2}{1 - \phi(1 - 2GM/R_{\text{core}}c^2)} \quad (13)$$

where

$$\phi \equiv \frac{(\alpha - 1)R_{\text{core}}c^2}{2GM}. \quad (14)$$

It should be noted that ϕ defined by Eq. (14) is a non-relativistic quantity and can be approximated for $\alpha \rightarrow 1$ by:

$$\phi \simeq \frac{\delta\mu R_{\text{core}}}{GMm_0} \quad \delta\mu = \mu_{\text{cc}} - \mu_0 \quad (15)$$

The numerical formula writes then:

$$\phi \simeq 7.27 \times 10^{-3} \left(\frac{\delta\mu}{\text{MeV}} \right) \left(\frac{R_{\text{core}}}{10 \text{ km}} \right) \left(\frac{M}{M_{\odot}} \right)^{-1}. \quad (16)$$

The leading term in the expansion of the right-hand-side of Eq. (13) in powers of the parameter ϕ gives an approximate formula for the thickness of the crust proportional to $\delta\mu$:

$$l_{\text{crust}} \simeq 1.82 \text{ km} \cdot \left(1 - \frac{2GM}{R_{\text{core}}c^2} \right) \left(\frac{\delta\mu}{25 \text{ MeV}} \right) \times \left(\frac{R_{\text{core}}}{10 \text{ km}} \right)^2 \left(\frac{M}{M_{\odot}} \right)^{-1} \quad (17)$$

where $\delta\mu$ is normalized to the “typical” value for the NS crust ($\sim 25 \text{ MeV}$, see Table 1). It should be however mentioned that for astrophysically relevant NS parameters ($M \sim 1 - 2 M_{\odot}$, $R_{\text{core}} \sim 10 - 12 \text{ km}$) one gets ϕ of the order of $0.15 - 0.25$. Therefore, ϕ cannot be considered as a very small number. Thus the accuracy of the expansion given by Eq. (17) is $\sim 20\%$ (see Fig. 6) and one should instead use the formula in Eq. (13) to determine the thickness of the crust with a high accuracy ($< 1\%$).

2.2. Approximate formula for the mass of the neutron-star crust

The crust contributes to the total mass of a NS. However the role of the mass of the crust for the total stellar mass is by one order of magnitude smaller than the importance of the crust thickness for the radius of a NS. To estimate the total mass of a NS with an accuracy similar to the one obtained using the approximation in Eq. (11) for the radius,

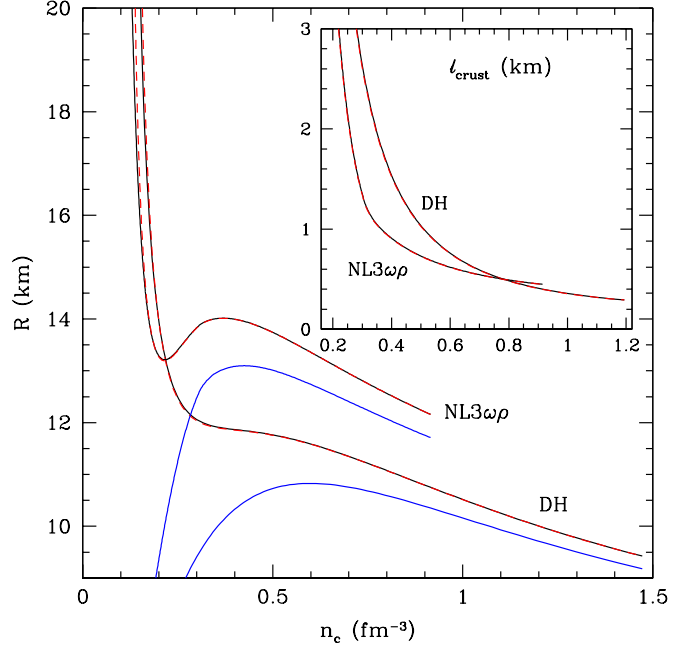


Fig. 1. NS radius R and thickness of the crust l_{crust} (inset) for the DH and NL3 $\omega\rho$ EOS as a function of the baryon density n_c at the center of the star. Solid (black) curves - exact solution calculated for the unified EOS (i.e. including the crust EOS), blue curves - radius of the core (above P_{cc}), dashed (red) lines - approximation based on Eq. (11), obtained using the core EOS only.

we can safely use a very crude approximation for the crust mass:

$$\frac{dP}{dm} = -\frac{GM}{4\pi r^4(1 - 2GM/rc^2)} \quad (18)$$

obtained from the TOV equation by neglecting the P/c^2 terms.

The mass of the crust is given by the formula:

$$M_{\text{crust}} = \frac{4\pi P_{\text{cc}} R_{\text{core}}^4}{GM_{\text{core}}} \left(1 - \frac{2GM_{\text{core}}}{R_{\text{core}}c^2} \right) \quad (19)$$

and is proportional to the pressure at the bottom of the crust P_{cc} . The total mass of the star is then $M = M_{\text{crust}} + M_{\text{core}}$.

Numerically:

$$M_{\text{crust}} \simeq 7.62 \times 10^{-2} M_{\odot} \cdot \left(\frac{P_{\text{cc}}}{\text{MeV fm}^{-3}} \right) \times \left(1 - \frac{2GM_{\text{core}}}{R_{\text{core}}c^2} \right) \left(\frac{R_{\text{core}}}{10 \text{ km}} \right)^4 \left(\frac{M_{\text{core}}}{M_{\odot}} \right)^{-1}. \quad (20)$$

3. Neutron-star parameters for a catalyzed crust

3.1. Mass and radius of a neutron star from μ_{cc}/μ_0

The approximate formulas presented in the previous section allow us to determine the main parameters of a NS (total mass, radius, crust thickness and mass) on the basis of the properties of its core only, i.e. using only an EOS $P(\rho)$ for nuclear matter below the crust/core interface (for $P > P_{\text{cc}}$). The only additional information required is the chemical

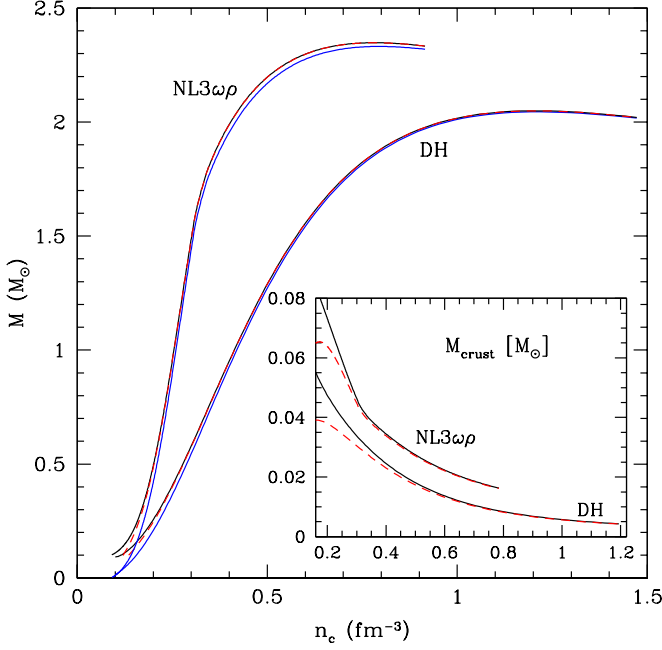


Fig. 2. NS mass M and mass of the crust M_{crust} (inset) for the DH and NL3 $\omega\rho$ EOS as a function of the baryon central density n_c . Solid (black) curves - exact solution calculated for the unified EOS (including the crust EOS), blue curves - mass of the core ($P > P_{\text{cc}}$), dashed (red) lines - approximation based on Eq. (19), obtained using the core EOS only.

Table 1. Crust/core boundary for the two considered EOS DH and NL3 $\omega\rho$ - the crust parameters for these EOSs are presented in Figs. 1-3. The bottom part of the table presents the artificial locations of the crust/core boundary used to test the accuracy of the approximate approach in Figs. 4, 5.

EOS	n_{cc} [fm $^{-3}$]	P_{cc} [MeV fm $^{-3}$]	μ_{cc} [MeV]
real crust/core location			
DH	0.077	0.335	953.3
NL3 $\omega\rho$	0.084	0.522	954.6
artificial crust/core location			
DH1	0.09	0.477	955.0
DH2	0.11	0.793	958.2
DH3	0.13	1.245	961.9
DH4	0.16	2.243	968.8

potential at zero pressure μ_0 . For cold catalysed matter the minimum energy is obtained for iron ^{56}Fe : $m_0 c^2 = \mu_0 = 930.4 \text{ MeV}$ (Haensel et al. 2007).

First, for a given central density n_c (or equivalently pressure P_c , given by the core EOS), and a chosen location of the core-crust transition at a density n_{cc} or pressure P_{cc} , the relation between the mass and radius of the NS core

$M_{\text{core}}(R_{\text{core}})$ is obtained by integrating the TOV equations outwards from the center of a star with $P = P_c$ down to P_{cc} . Then the mass of the crust M_{crust} is determined using Eq. (19) and consequently so is the total mass of the star M . Using Eq. (11) the canonical $M(R)$ relation between the mass and the radius of the NS is reconstructed. The thickness of the crust is finally given by Eq. (13).

In Figs. 1, 2 we present the result of a such procedure for two models of dense matter fulfilling the observational constraint on the maximum allowable mass $M_{\text{max}} > 2 M_{\odot}$: DH (Douchin & Haensel 2001) and the stiffer NL3 $\omega\rho$ (Fortin et al. 2016). The approximate solution (dashed lines) is almost undistinguishable from the exact one except in the region of relatively small central density. Similar conclusions are obtained for the parameters of the crust (thickness and mass) presented in the insets. In Fig. 3 various relations between masses and radii are presented. The black solid lines are the $M(R)$ relations obtained when solving the TOV equations in the whole NS (core and crust) with a unified EOS, i.e. when the same nuclear models for the crust and the core are used. The blue solid lines correspond to the dependence $M_{\text{core}}(R_{\text{core}})$ and are obtained solving the TOV equations in the core i.e., from the center at pressure P_c outwards to the pressure at core/crust interface P_{cc} . The red dashed lines are obtained using the $M(R_{\text{core}})$ relations in Eq. (11). In the latter case, we do not need any information about the crust EOS except the chemical potentials at zero pressure μ_0 and at the bottom of the crust μ_{cc} in order to determine the total radius of the star. For a chosen value of the density at the core-crust transition (see Sect. 3.2) μ_{cc} can be calculated from Eq. (6) using the core EOS.

The approximate formula Eq. (11) works very well for astrophysically interesting masses of NS: $M > 1 M_{\odot}$. For the sake of completeness, let us mention that for masses as small as $0.2 M_{\odot}$ the validity of the formula breaks down, because the condition $M_{\text{crust}} \ll M$ is then obviously not fulfilled. For the NL3 $\omega\rho$ EOS the difference between the exact and approximate radii is 20 m ($1.0 M_{\odot}$), 8 m ($1.5 M_{\odot}$) and 3 m ($2.0 M_{\odot}$). Therefore, for $M > 1 M_{\odot}$ the relative error is less than 0.15% of the radius of a star (or less than 1% of the thickness of the crust). For the DH EOS the accuracy of the approximate approach is even better. For the estimation of the mass of the crust we use the simplest approximations in Eq. (20) which is accurate up to 6% for $M > 1 M_{\odot}$ therefore resulting in a very small error in the total mass determination (less than 0.3%).

3.2. Choice of the core-crust transition

At the core-crust interface the ground state of neutron star matter changes from a lattice of spherical nuclei in the solid crust to homogeneous matter in the liquid core. Some models predict the appearance of so-called pasta phases when the most stable shape of nuclei is not any more a sphere but, as the density increases, a rod or a slab immersed in the neutron gas (Ravenhall et al. 1983). Various approaches have been developed to determine the density of the core-crust transition n_{cc} eg. the study of thermodynamic spinodal or dynamical spinodal surfaces, Thomas Fermi calculations or the Random Phase Approximation. However for β -equilibrated matter, the values of n_{cc} that are obtained have been shown to be similar (see for exam-

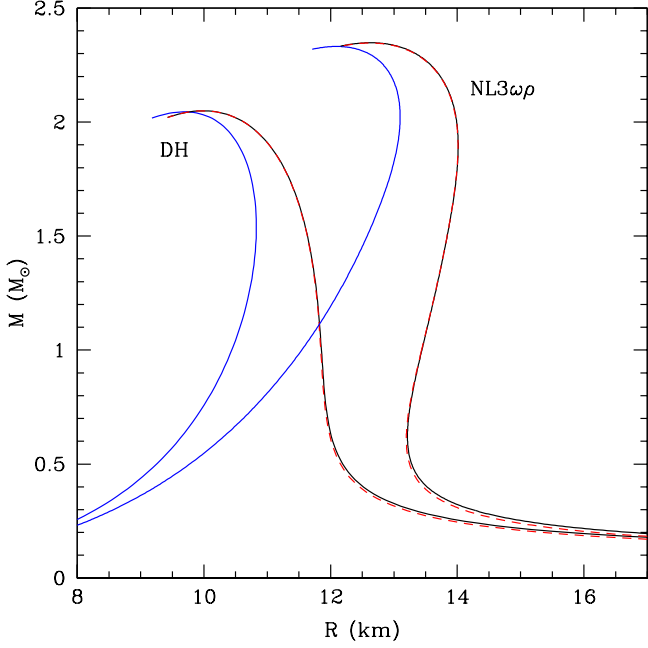


Fig. 3. $M(R)$ dependence for the exact solution of the TOV equations obtained using a unified EOS and for our approximate approach, for the DH and NL3 $\omega\rho$ models of dense matter. Solid (black) curves - $M(R)$ calculated with a unified EOS, solid (blue) curves - $M_{\text{core}}(R_{\text{core}})$ relation, dashed (red) lines - $M(R)$ approximation based on Eq. (11)-(12), and the black ones - the exact solution of the TOV equation.

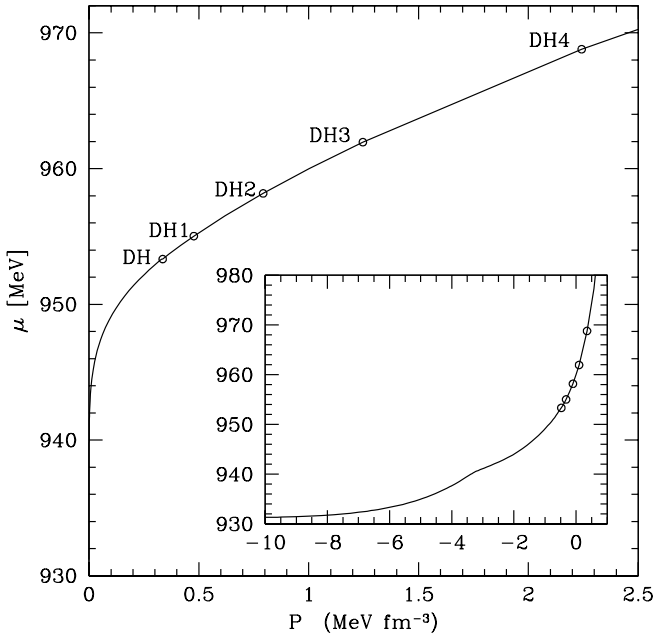


Fig. 4. Baryon chemical potential μ as a function of the pressure for the DH EOS. The points mark the value of the chemical potential at various assumed locations for the core-crust boundary used in Eq. (11)-(12) and presented in Table 1. The lowest point (DH) corresponds to the real core-crust interface in the DH model. Inset: $\mu(P)$ in logscale for the pressure.

ple Horowitz & Shen (2008); Avancini et al. (2010, 2012); Pais et al. (2016) and references therein).

The transition density is inversely proportional to the slope of the symmetry energy L (Horowitz & Piekarewicz 2001) and for typical values of $30 \leq L \leq 120$ MeV, Ducoin et al. (2011) find for a large set of EOS based on two nuclear approaches to the many-body problem (Skyrme models and Relativistic Mean Field calculations) $0.06 \leq n_{\text{cc}} \leq 0.10 \text{ fm}^{-3}$ or $0.38 \leq n_{\text{cc}}/n_0 \leq 0.63$. Consequently, if for a given core EOS no calculation of the core-crust transition density is available, taking $n_{\text{cc}} = 0.5n_0$ appears reasonable.

In this subsection we discuss the accuracy of our approximate approach to calculate the main parameters of a NS for different given locations of the crust-core boundary, using the DH model of dense matter as an example. In this model the ‘real’ crust-core boundary is located at $n_{\text{cc}} = 0.077 \text{ fm}^{-3}$, i.e. at about half nuclear matter density. To test the dependence of our approximations on n_{cc} we artificially re-define the location of the core boundary to 0.09, 0.11, 0.13, 0.16 fm^{-3} (models DH1-DH4 in Table 1). The size of the core, which is defined by the pressure P_{cc} , decreases with increasing P_{cc} and is smallest (at given central pressure P_c) for the DH4 model. Consequently the region of the star described by the approximate formulas (outer part $P < P_{\text{cc}}$) is larger for larger P_{cc} and for the DH4 model (with $n_{\text{cc}} \simeq n_0$) the mass of the crust is about $0.1 M_{\odot}$, which is much larger than the mass of the real crust (unified DH EOS, $< 0.02 M_{\odot}$).

Fig. 4 shows the baryon chemical potential μ as a function of the pressure P for the DH EOS of the core. The dots correspond to the considered crust/core location (see Table 1). The lowest value is the real density of the crust-core interface for the (unified) DH model.

In Fig. 5 we present the results of our approximate approach given by Eq. (11)-(12) for the mass-radius relation for the DH EOS. For the real value of n_{cc} the difference between the exact and approximate results is 30 m at $M = 0.5 M_{\odot}$, 10 m at $M = 1 M_{\odot}$ and less than 4 m at $M = 1.5 - 2 M_{\odot}$. Even for an unrealistically large value of $n_{\text{cc}} = n_0 = 0.16 \text{ fm}^{-3}$ (DH4) the approximation gives a quite high accuracy with the uncertainty on R decreasing from ~ 100 m at $1 M_{\odot}$ down to 30 m at $1.5 M_{\odot}$ and 5 m at $2 M_{\odot}$.

The accuracy of the approximate approach for the thickness and mass of the crust is presented in Fig. 6 for three different locations of the bottom of the crust (models DH, DH2, DH4). The thickness of the crust is determined very accurately by the formula (13). The relative error is less than 0.7% for DH and $< 3.5\%$ for DH4 which is equivalent to < 10 m and < 100 m inaccuracy (i.e. 0.08%, 0.7% error in the radius of the star R). Although for the presented range of masses from $1 M_{\odot}$ to M_{max} the maximum relative error in M_{crust} is 5-8%, the determination of the total mass M of neutron star is very accurate (1% for $n_{\text{cc}} = n_0$ and 0.1% for $n_{\text{cc}} = 0.5n_0$ at $M = 1 M_{\odot}$, the error decreasing rapidly with further increase of M).

3.3. Accuracy of the approximate approach and crust/core matching problem

In the case of a non-unified EOS the matching of the core EOS to the crust EOS is often performed by an artificial

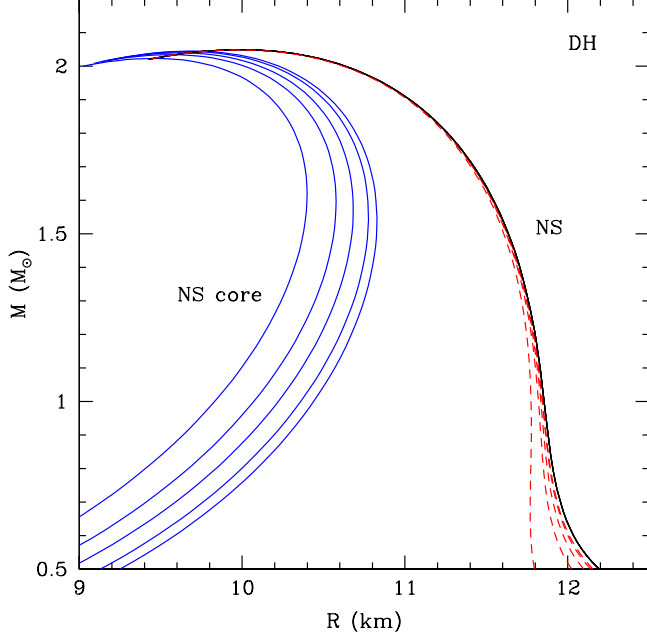


Fig. 5. $M(R)$ dependence for the exact solution of the TOV equations obtained using a unified EOS and the approximate approach for the DH EOS. Different values of n_{cc} are used (from left to right; $0.16, 0.13, 0.11, 0.09, 0.077 \text{ fm}^{-3}$, see Table 1 for details). The value $n_{cc} = 0.077 \text{ fm}^{-3}$ corresponds to the ‘real’ crust/core boundary for the DH model. The solid blue curves show the $M(R_{\text{core}})$ relation, the dashed red ones the $M(R)$ approximation based on Eq. (11)-(12) and the black one the exact solution of the TOV equation.

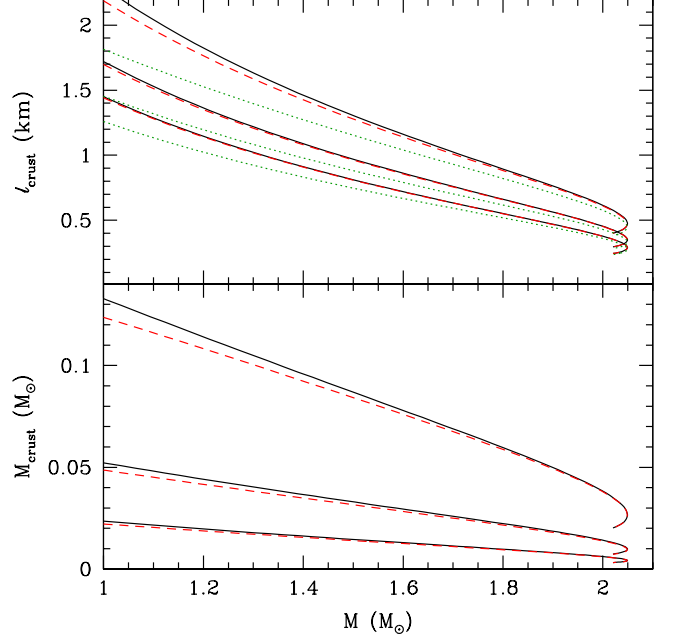


Fig. 6. Thickness l_{crust} (upper panel) and mass M_{crust} (lower panel) of the crust of a NS for the DH EOS and for different values of n_{cc} (from top to bottom; $0.16, 0.11, 0.077 \text{ fm}^{-3}$). The density $n_{cc} = 0.077 \text{ fm}^{-3}$ corresponds to the crust/core boundary for the DH model. Solid lines - exact results calculated for the complete EOS (including the crust EOS), dashed (red) lines - approximations based on Eq. (13) (thickness) and Eq. (19) (mass), dotted (green) lines - linearisation Eq. (17) of Eq. (13).

function $P(\rho)$ or $P(n)$ (which can be linear, polytropic, ...). In general this approach leads to thermodynamic inconsistency, which manifests itself in a discontinuity in μ (for details see Fortin et al. 2016). This discontinuity $\delta\mu_{\text{EOS}}$ can be as high as few MeV, but is usually of the order of $\delta\mu_{\text{EOS}} \simeq 0.5 - 1.5 \text{ MeV}$. It results in an error in the crust thickness determination which can be calculated with Eq. (17). The relative error in l_{crust} is then proportional to $\delta\mu_{\text{EOS}}/\Delta\mu$ where $\Delta\mu$ is the chemical potential range in the crust (20-30 MeV). For example, for $\delta\mu_{\text{EOS}} \simeq 1 \text{ MeV}$ the error due to inconsistent crust/core matching is larger than the accuracy given by our approximation for the crust thickness (for $n_{cc} = 0.5 n_0$ and $M = 1.4 M_{\odot}$ it is 40 m. compared to 5 m inaccuracy of our model).

As a consequence, using the approximate formula for the radius: Eq. (11) and the crust thickness: Eq. (13) and mass: Eq. (19), without any further knowledge about the crust EOS, is in general more accurate than the widely-used method of matching in a thermodynamically inconsistent way an EOS for the crust to a different (non-unified) one for the core.

4. Accreted vs catalyzed crust

A characteristic feature of the EOS for an accreted crust is the existence of energy sources at pressures at which exothermic nuclear reactions are induced by the accretion of matter onto the NS surface. As a result the $\mu(P)$ relation

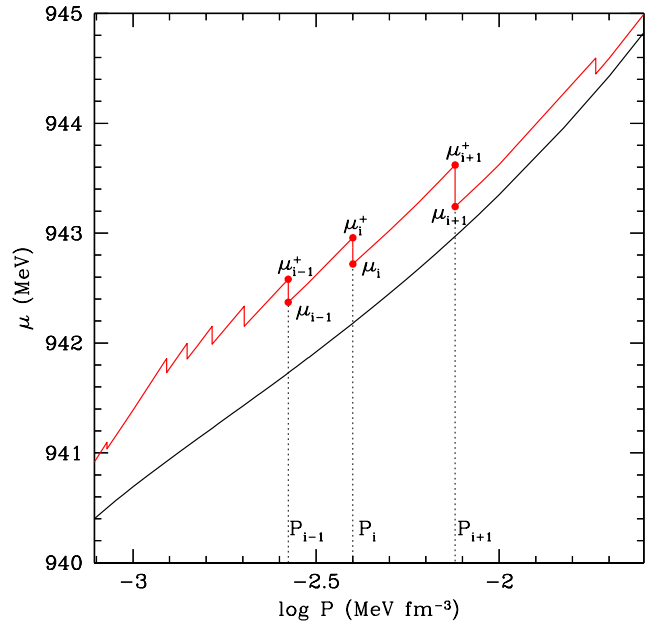


Fig. 7. Baryon chemical potential μ for catalyzed (lower curve) and accreted crust (step-like curve). The Mackie & Baym (1977) model of dense matter is used in the example (for details see Haensel & Zdunik (2008)).

is a discontinuous function with drops in μ equal to the energy release per one accreted nucleon. In Fig. 7 we present an example for the Mackie & Baym (1977) model of dense matter (Haensel & Zdunik 2008) of a continuous $\mu^{(\text{GS})}(P)$ dependence for catalyzed matter (lower continuous curve which corresponds to the minimum value of μ at a given pressure) and for an accreted crust (with energy sources located at $P = P_{i-1}, P_i, P_{i+1}$).

4.1. Thickness of an accreted crust

In Sect. 2 we considered a catalysed crust for which the function $\mu(P)$ is continuous and Eqs. (6,7) hold. In this case the formula (8) can be used for the whole crust, resulting in Eq. (13). In the case of an accreted crust, $\mu(P)$ is not continuous as shown in Fig. 7 and each jump in the chemical potential at a fixed pressure corresponds to an energy source. Consequently, in order to determine the thickness of an accreted crust one has to calculate separately the thickness of each shell located between two energy sources, for example between P_{i-1} and P_i as plotted in Fig. 7.

Using Eq. (8) the following set of equations is obtained:

$$\begin{aligned} \frac{\sqrt{1 - \frac{2GM}{Rc^2}}}{\sqrt{1 - \frac{2GM}{R_1c^2}}} &= \exp \chi_1 = \frac{\mu_1^+}{\mu_0} \\ \frac{\sqrt{1 - \frac{2GM}{R_1c^2}}}{\sqrt{1 - \frac{2GM}{R_2c^2}}} &= \exp \chi_2 = \frac{\mu_2^+}{\mu_1} \\ &\dots \\ \frac{\sqrt{1 - \frac{2GM}{R_ici^2}}}{\sqrt{1 - \frac{2GM}{R_{i+1}c^2}}} &= \exp \chi_{i+1} = \frac{\mu_{i+1}^+}{\mu_i} \\ &\dots \\ \frac{\sqrt{1 - \frac{2GM}{R_n c^2}}}{\sqrt{1 - \frac{2GM}{R_{\text{core}}c^2}}} &= \exp \chi_{n+1} = \frac{\mu_{\text{core}}^+}{\mu_n} \end{aligned}$$

where the subscript ‘core’ corresponds to the convergence point of the baryon chemical potential for accreted and catalyzed crusts at the bottom of the crust, i.e. where the condition $\mu_{\text{core}}^+ = \mu_{\text{core}}$ is fulfilled (see Fig. 7).

Multiplying the above equations by one another we get the final formula for the thickness of an accreted crust:

$$\begin{aligned} \frac{\sqrt{1 - \frac{2GM}{Rc^2}}}{\sqrt{1 - \frac{2GM}{R_{\text{core}}c^2}}} &= \frac{\mu_1^+}{\mu_1} \cdot \frac{\mu_2^+}{\mu_2} \dots \frac{\mu_i^+}{\mu_i} \dots \frac{\mu_n^+}{\mu_n} \cdot \frac{\mu_{\text{core}}}{\mu_0} \\ &= \frac{\mu_{\text{core}}}{\mu_0} \cdot \prod_{i=1}^n \frac{\mu_i^+}{\mu_i} \end{aligned} \quad (21)$$

where the product is calculated over all the energy sources in the accreted crust.

The energy release per one accreted nucleon at the pressure P_i is given by $Q_i = \mu_i^+ - \mu_i$. Because $Q_i/\mu_i < 10^{-3}$, one can safely approximate formula Eq. (21) by

$$\frac{\sqrt{1 - \frac{2GM}{Rc^2}}}{\sqrt{1 - \frac{2GM}{R_{\text{core}}c^2}}} \simeq \frac{\mu_{\text{core}}}{\mu_0} \left(1 + \sum_{i=1}^n \frac{Q_i}{\mu_i} \right). \quad (22)$$

The main energy sources for an accreted crust are located in the inner crust at typical pressures $P \sim 0.001 - 0.01 \text{ MeV fm}^{-3}$ ($10^{30} - 10^{31} \text{ erg cm}^{-3}$) where the chemical potential $\mu_{\text{IC}} \simeq 942 \text{ MeV}$. Replacing μ_i in Eq. (22) by this typical value, we get:

$$\frac{\sqrt{1 - \frac{2GM}{Rc^2}}}{\sqrt{1 - \frac{2GM}{R_{\text{core}}c^2}}} \simeq \frac{\mu_{\text{core}}}{\mu_0} \left(1 + \frac{Q_{\text{tot}}}{\mu_{\text{IC}}} \right) \quad Q_{\text{tot}} = \sum_{i=1}^n Q_i, \quad (23)$$

where Q_{tot} is the total energy release in the crust.

4.2. Thickness of a catalyzed crust vs. an accreted one

The formulas for the radius R_{cat} and R_{acc} of a NS with a catalysed crust and an accreted one, respectively, are:

$$\frac{\sqrt{1 - \frac{2GM}{R_{\text{cat}}c^2}}}{\sqrt{1 - \frac{2GM}{R_{\text{core}}c^2}}} = \frac{\mu_{\text{core}}}{\mu_0}, \quad (24)$$

$$\frac{\sqrt{1 - \frac{2GM}{R_{\text{acc}}c^2}}}{\sqrt{1 - \frac{2GM}{R_{\text{core}}c^2}}} = \frac{\mu_{\text{core}}}{\mu_0} \cdot \prod_{i=1}^n \frac{\mu_i^+}{\mu_i}. \quad (25)$$

They are equivalent to:

$$\frac{\sqrt{1 - \frac{2GM}{R_{\text{acc}}c^2}}}{\sqrt{1 - \frac{2GM}{R_{\text{cat}}c^2}}} = \prod_{i=1}^n \frac{\mu_i^+}{\mu_i} \simeq 1 + \frac{Q_{\text{tot}}}{\mu_{\text{IC}}}. \quad (26)$$

Defining $\sqrt{\alpha} \equiv \prod_{i=1}^n \frac{\mu_i^+}{\mu_i}$, Eq. (11) holds with R and R_{core} replaced by R_{acc} and R_{cat} respectively, i.e.:

$$\frac{R_{\text{cat}}}{R_{\text{acc}}} = 1 - (\alpha - 1) \left(\frac{R_{\text{cat}}c^2}{2GM} - 1 \right). \quad (27)$$

The difference in the radii of NS with an accreted crust and with a catalyzed one: $\Delta R = R_{\text{acc}} - R_{\text{cat}}$ is small compared to R and one gets the approximate relation:

$$\frac{\Delta R}{R_{\text{cat}}} \simeq \left[\left(\prod_{i=1}^n \frac{\mu_i^+}{\mu_i} \right)^2 - 1 \right] \left(\frac{R_{\text{cat}}c^2}{2GM} - 1 \right). \quad (28)$$

Using Eq. (26) we obtain:

$$\frac{\Delta R}{R_{\text{cat}}} \simeq 2 \left(\frac{R_{\text{cat}}c^2}{2GM} - 1 \right) \sum_{i=1}^n \frac{Q_i}{\mu_i} \simeq 2 \frac{Q_{\text{tot}}}{\mu_{\text{IC}}} \left(\frac{R_{\text{cat}}c^2}{2GM} - 1 \right) \quad (29)$$

which, after normalization to typical values, becomes:

$$\Delta R \simeq 144 \text{ m} \cdot \left(\frac{Q_{\text{tot}}}{2 \text{ MeV}} \right) \left(\frac{R_{\text{cat}}}{10 \text{ km}} \right)^2 \left(\frac{M}{M_{\odot}} \right)^{-1} \left(1 - \frac{2GM}{R_{\text{cat}}c^2} \right), \quad (30)$$

where we used $\mu_{\text{IC}} = 942 \text{ MeV}$. The inaccuracy of the formula (30) introduced by the approximations (22,23,29) is of the order of $(Q_{\text{tot}}/940 \text{ MeV})$, about 0.1% in ΔR (i.e. much less than 1 meter).

The accuracy of our approximation is visualized in Fig. 8. The exact $M(R)$ curve is obtained for the DH EOS with catalysed and accreted crusts based on

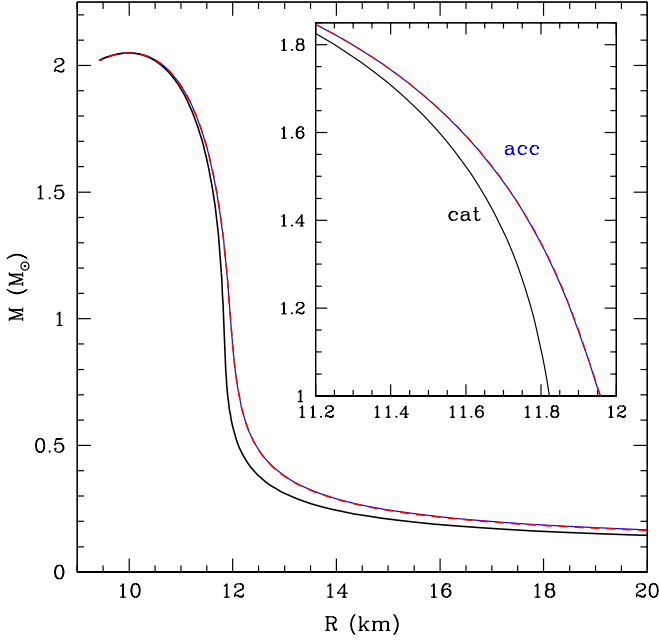


Fig. 8. Mass-radius relation for the DH EOS for catalyzed (black, solid curve) and accreted crusts (blue, solid line). The approximation given by Eq. (30) is plotted by a dashed red curve which can be hardly distinguished from the exact result for an accreted crust. Inset - zoom for masses 1 – 2 M_{\odot} .

Mackie & Baym (1977) model of nuclei (Zdunik & Haensel 2011; Haensel & Zdunik 2008). The difference in radii due to the formation scenario (ie. accreted vs. catalyzed matter) is $\Delta R = 80$ m for $1.4 M_{\odot}$ and in the range 330 – 50 m for masses between $0.5 M_{\odot}$ and $1.8 M_{\odot}$ respectively. For the considered model of accreted matter the total energy release is $Q_{\text{tot}} = 1.9 \text{ MeV}$ and the $M(R)$ dependence obtained using Eq. (30) nearly coincides with the exact one, with a difference of about 1 m for $M = 1.5 M_{\odot}$.

Let us mention that when deriving Eqs. (24,25) we assume the same value of μ_{core} and μ_0 for both an accreted crust and a catalyzed one. For μ_{core} this assumption is justified; indeed the baryon chemical potential μ for catalyzed and accreted crusts converges at pressures larger than $\sim 0.03 \text{ MeV fm}^{-3}$ (see Fig. 7). However for an accreted crust the value of μ_0 actually depends on the ashes of nuclear reactions at the surface of the NS (as a result of the X-ray bursts, Haensel & Zdunik 2003). In principle it is possible that $\mu_{0\text{acc}} \neq \mu_{0\text{cat}}$ and the product $\prod_{i=1}^n \frac{\mu_i^+}{\mu_i^-}$ should then be multiplied by $\mu_{0\text{acc}}/\mu_{0\text{cat}}$. In practice the difference is smaller than 0.2 MeV/nucleon (0.02%) for the ashes considered by Gupta et al. (2007); Haensel & Zdunik (2008).

5. Conclusions

In this paper we present an approximate treatment for the crust of a NS which allows to calculate the mass and radius of a NS, the crust thickness and the crust mass. Two limiting cases were considered: catalyzed (ground-state) crust and fully accreted crust. For a catalyzed crust R , l_{crust} , M_{crust} , and M do not depend on the specific form of the crust EOS, but on the crust-core transition density only and

on the EOS core. For a given core EOS and chosen density at which the core-crust transition takes place, the relation between the core radius and mass is obtained by solving the TOV equations. Then the mass and radius of the crust and the total mass and radius of the star can be obtained using simple formulas. The accuracy of this approach is higher than 1% and 5% for l_{crust} and M_{crust} respectively, for NS masses larger than $1 M_{\odot}$. This is equivalent to the determination of global parameters of NS (radius R and mass M) with maximum error $\sim 0.1 - 0.3\%$. Notice that unless if available in the literature, for a given EOS of the core, the transition density n_{cc} between the core and the crust is not known in advance. However for reasonable values of the symmetry energy usually $n_{\text{cc}} \simeq 0.5 n_0$. A simple and accurate formula for the difference in the radii of a NS with a fully accreted crust with respect to one with a catalyzed crust is derived. It is proportional to the total energy release due to deep crustal heating and depends in addition only on the mass and radius of the model with a catalyzed crust.

The demonstrated high precision of the prediction of the radius of a NS makes the derived formulas of interest for theoretical works in particular in relation with the next generation of X-ray telescopes which are expected to provide measurements of the NS radius with a precision of few percent.

Acknowledgements. This work was partially supported by the Polish National Science Centre (NCN) grant no. 2013/11/B/ST9/04528 and the COST Action NewCompStar. MF would like to thank Constana Providência for useful discussions. We also acknowledge helpful remarks of participants of the MODE-SNR-PWN 2016 Workshop (Meudon, France), after the talk by one of the authors (MF).

References

- Arzoumanian, Z., Gendreau, K. C., Baker, C. L., Cazeau, T., Hestnes, P., et al. 2014, Proc. SPIE 9144, Space Telescopes and Instrumentation 2014: Ultraviolet to Gamma Ray, 914420.
- Avancini, S. S., Chiacchiera, S., Menezes, D. P., & Providência, C. 2010, Phys. Rev. C, 82, 055807
- Avancini, S. S., Chiacchiera, S., Menezes, D. P., & Providência, C. 2012, Phys. Rev. C, 85, 059904
- Brown E. F., Bildsten L., Rutledge R. E., 1998, Astrophys. J. Lett., 504, L95
- Chamel, N., Haensel, P. 2008, Living Reviews in Relativity, 11, no.10
- Chamel, N., Fantina, A.F., Zdunik, J.L., Haensel, P. 2015, Phys. Rev. C, 91, 055803
- Douchin, F., & Haensel, P. 2001, A&A, 380, 151
- Ducoin, C., Margueron, J., Providência, C., & Vidaña, I. 2011, Phys. Rev. C, 83, 045810
- Fantina, A. F., Chamel, N., Pearson, J. M., & Goriely, S. 2013, A&A, 559, A128
- Feroci, M., den Herder, J. W., Bozzo, E., et al. 2012, Proc. SPIE, 8443, 84432D
- Fortin, M., Providência, C., Raduta, A. R., et al. 2016, Phys. Rev. C, 94, 035804
- Goriely, S., Chamel, N., Pearson, J.M, Phys. Rev. C, 82, 035804 (2010)
- Gupta, S., Brown, E. F., Schatz, H., Miller, P., & Kratz, K.-L. 2007, ApJ, 662, 1188
- Haensel, P., Potekhin, A.Y., Yakovlev, D.G., 2007, Neutron Stars 1 Equation of state and structure (New York, Springer)
- Haensel, P., Zdunik, J. L., 1990, A&A, 227, 431
- Haensel, P., Zdunik, J. L., 2008, A&A, 404, L33
- Haensel, P., Zdunik, J. L., 2008, A&A, 480, 459
- Horowitz, C. J., & Piekarewicz, J. 2001, Physical Review Letters, 86, 5647
- Horowitz, C. J., & Shen, G. 2008, Phys. Rev. C, 78, 015801
- Lattimer, J., Prakash, M., 2007, Physics Reports 442, 109–165
- Lindblom, L, 1992, ApJ 398, 569
- Mackie, F.D, Baym, G., 1977, Nucl. Phys. A, 285, 332

- Motch, C., Wilms, J., Barret, D., et al. 2013, arXiv:1306.2334
- Pearson, J. M., Chamel, N., Fantina, A. F., & Goriely, S. 2014, European Physical Journal A, 50, 43
- Pais, H., Sulaksono, A., Agrawal, B. K., & Providência, C. 2016, Phys. Rev. C, 93, 045802
- Ravenhall, D. G., Pethick, C. J., & Wilson, J. R. 1983, Physical Review Letters, 50, 2066
- Zdunik, J. L. 2002, A&A, 394, 641
- Zdunik, J. L., Haensel, P., 2011, A&A, 530, A137
- Zdunik, J. L., Bejger, M., Haensel, P., 2008, A&A, 491, 489